

Weak Gravitational Lensing



Erik van der Bijl

Seminar Cosmology

February 21, 2009

Abstract

Weak gravitational lensing measurements shed a new light on the dark matter distribution in our universe. We present an introduction to weak lensing. Starting with a derivation of the deflection angle for a ray of light deflected by a point mass. Then by investigating the typical geometry of weak lensing we introduce the dimension-less surface mass density and the shear of the lensing mass distribution. We discuss and compare two methods to probe the mass distribution. The two methods are based respectively on shear and magnification by the lensing galaxy, we conclude that shear measurements give more significant results than magnification measurements. The end of this paper is dedicated to the discussion of two papers that used weak gravitational lensing measurements.

Contents

Introduction	2
Light Deflection	6
Point Mass	6
Galaxy–Galaxy lensing	7
Observables	12
Observations	23
Conclusions	27

Introduction

In 1933 the astronomer Fritz Zwicky studied the Coma Cluster of galaxies (Abell 1656). Using the virial theorem he was able to calculate the amount of mass from the rotation curves of the stars within the system. When he compared this mass to the mass that one could expect based on the amount of emitted light of the stars, he found a discrepancy. This led him to the conclusion that the Coma Cluster must contain a large amount of unseen matter, which he baptized dark matter. Although Zwicky was a well known astronomer his results were received with much skepticism. Forty years later the American astronomer Vera Rubin, revived Zwicky's dark matter hypothesis. Together with Kent Ford, who had developed an extremely sensitive spectrometer, she investigated the orbital velocities in spiral galaxies by looking at the Doppler shift of various stars. Still reluctantly the astronomical community accepted her results that established that there should be about ten times more mass in spiral galaxies than could be expected from luminosities.

The virial theorem of statistical mechanics gives the relation between the average total kinetic energy of a system of particles and its total potential energy. The virial theorem for a system of N -particles reads,

$$-2 \langle T \rangle = \left\langle \sum_{i=1}^N \mathbf{F}_i \cdot \mathbf{r}_i \right\rangle, \quad (1)$$

where T denotes the total kinetic energy within the system and \mathbf{F}_i is the total force on each particle at position \mathbf{r}_i . The brackets indicate an ensemble average. Since the virial theorem holds for stable bound systems, it also holds for equilibrated clusters of stars and galaxies. Using the Newtonian potential for the gravitational attraction we find,

$$\sum_{i=1}^N m_i v_i^2 = \frac{1}{2} \sum_i^N \sum_{j \neq i}^N G_N \frac{m_i m_j}{|r_i - r_j|}, \quad (2)$$

where the right hand side comes from the Newtonian potential energy, we also dropped the ensemble averages, assuming that the observed quantities

equal the ensemble averages. Due to the enormous distances in space, astronomers can only measure the radial component of the velocity of stars in this cluster. However, an astronomer on Earth is as likely to see a star moving in the radial direction as in either of the other two perpendicular directions. This leads to,

$$\langle v^2 \rangle = 3 \langle v_r^2 \rangle.$$

For simplicity we now assume that we are dealing with a spherical cluster of radius R with N stars, each with mass m . We obtain,

$$3m \langle v^2 \rangle \approx \frac{3 G_N N m^2}{5 R},$$

where we obtained the right hand side integrating a spherically symmetric constant density of stars. This approximation leads to the expectation that the physical mass is of the same order of magnitude[1]. From the above equation we finally arrive at,

$$\langle v^2 \rangle \approx \frac{G_N M_{viral}}{5R}. \quad (3)$$

Defining the viral mass as $M_{viral} = Nm$. Using this approach based on the virial theorem Zwicky was able to estimate that the observed mass of the Coma Cluster is an order of magnitude greater than the mass that was estimated using the luminosity of the stars.

There exists another approach to determine the mass of clusters of galaxies that is based on the notions of classical mechanics. This method also relies on measurements of the velocities of stars. This method, like Zwicky's method, also needs the assumption that the system under investigation is dynamically stable. We can use the luminous mass to calculate the rotational velocities of stars as predicted by the Newtonian gravitational potential. We can compare the calculated rotation curves to the values measured using Doppler shifts. We expect that the tangential velocity of a star is given by the relation,

$$v(r)^2 = \frac{G_N M_r}{r}, \quad (4)$$

where M_r denotes the amount of luminous mass within a sphere of radius r . For typical spiral galaxies most of the mass is situated close to the center. This allows us to expect that the stars in the spiral arms have a velocity distribution $v(r) \propto r^{-1/2}$. In contrast to this the measurements of the Doppler shifts of various stars in numerous systems show flat rotational curves, $v(\vec{r}) \propto \text{constant}$. This discrepancy can be used to infer that there should be dark matter halos surrounding the centers of galaxies.



Figure 1: Abell 2218. In this cluster giant luminous arcs can be seen. This Hubble Space Telescope image shows a collection of distorted galaxy images tangentially aligned with respect to the cluster center.

The developments of cosmology in the last century give another reason to embrace the dark matter hypothesis. Measurements on standard candles as well as measurements on the cosmic microwave background (CMB) radiation, together with the Friedmann–Lemaître–Robertson–Walker metric have created the standard model of cosmology. Within this model dark matter is quite abundant in our universe. For a detailed account how the dark matter density depends on the CMB anisotropies see [3]. Although the evidence that supports the dark matter hypothesis is rather strong and accepted, there are some physicists that have a phenomenological theory that modifies Newton’s gravitational law. This theory called modified Newtonian dynamics (MOND) assumes that Newton’s second law is incorrect for small accelerations. For a review see Bekenstein [4], or Rot [5]. Rotation curves can be fitted by MOND using only one parameter, whereas dark matter needs a whole distribution of dark matter in each cluster. This report introduces another method to search for the dark matter in our universe using a more direct method than the virial measurements, rotation curves or the CMB anisotropies. This method is based on light deflection by mass, gravita This report focuses on weak gravitational lensing. Weak lensing is well understood within general relativity and is possible with the current telescope techniques. We start with a derivation of the deflection of light by a point mass. Then we proceed with the introduction of the dimension–less surface mass density and the components of shear. These quantities describe how a mass distribution deflects light, but we need to inverse this result, because we only have access to the deflected images. When we perform shear anal-

ysis this inversion is based on the assumption that all galaxy images can be approximated by ellipses with a random orientation. When we use the number density of the source galaxies to determine the mass distribution we need to compare our measured field to a non-lensed field of source galaxies. Both methods are discussed and compared. In the last part of this paper we will discuss two papers that used weak lensing to support the dark matter hypothesis, and study its distribution in our universe.

Light deflection

This chapter introduces weak gravitational lensing. It starts with a derivation of the deflection of light by a stationary mass distribution. This result will then be used to introduce the deflection potential which is used in recent observations to study the distribution of dark matter in our universe. When the necessary derivations are done, we turn our attention to those observations. In the following section we follow Prokopec[6]. The second section is based on reviews[9][10][12].

Point-like Mass

In order to be able to study weak gravitational lensing we should start with the deflection of light by a spherically symmetric mass distribution M . Our starting point will be the relativistic action for a point particle with mass m ,

$$S = mc \int ds = \int L dt, \quad L = mc \sqrt{g_{\mu\nu} \frac{dx^\mu}{dt} \frac{dx^\nu}{dt}}. \quad (5)$$

Using the canonical framework we can easily obtain the momentum $p^\mu = \frac{\partial L}{\partial(dx^\mu/dt)}$. This leads to the Euler-Lagrange equation,

$$\frac{dp_\nu}{dt} = \frac{1}{2} \partial_\nu g_{\alpha\beta} p^\alpha \frac{dx^\beta}{dt}. \quad (6)$$

Now we are going to use that photons are massless. This implies for photons that $g_{\mu\nu} p^\mu p^\nu = 0$. This algebraic constraint on the 4-momentum allows us to determine the photons dispersion relation $p^0(p^i)$. Since we are interested in weak lensing, it suffices to work with a metric that is given by a Newtonian diagonal form,

$$ds^2 = \left(1 + \frac{2\phi_N}{c^2}\right) dt^2 - \left(1 - \frac{2\phi_N}{c^2}\right) \delta_{ij} dx^i dx^j. \quad (7)$$

Where ϕ_N is the Newtonian potential of a quasi stationary mass distribution. Equation (6) now implies the conservation of canonical energy $E = p_0/c$,

$$\frac{dp^0}{dt} = \frac{d}{dt} \left(\left(1 + 2\frac{\phi_N}{c^2}\right) p^0 \right) = 0. \quad (8)$$

for the spatial components we obtain, again using (6),

$$\frac{dp^i}{dt} = -\frac{d}{dt} \left(\left(1 - 2\frac{\phi_N}{c^2}\right) p^i \right) = \frac{c}{2} \partial_i g_{\alpha\beta} \frac{p^\alpha p^\beta}{p^0}. \quad (9)$$

When we divide this equation by the constant factor, $-(1 + 2\phi_N/c^2)(p^0/c)$, we find after some algebra,

$$\frac{d}{dt} \left(\left(1 - 4\phi_N/c^2\right) \frac{d\vec{x}}{dt} \right) = -2\nabla\phi_N. \quad (10)$$

This relation implies that for relativistic moving bodies the gravitational field appears to be a factor two larger than what one would expect from the Newtonian limit for small velocities. When the light bending angle $\hat{\alpha}$ is small, we can make the approximation,

$$\frac{d\vec{x}(y)}{dt} = -\frac{2}{c} \int_{y_S}^y dy' \nabla'_\perp \phi_N, \quad (11)$$

where the photon is moving from a source S in the y direction at the speed of light. The light bending angle $\hat{\alpha}$ can now be written as,

$$\hat{\alpha} = -\frac{2}{c^2} \int_{y_S}^{y_O} dy \partial_x \phi_N. \quad (12)$$

For a point-like mass M at the origin we have a Newtonian potential $\phi_N(r) = -G_N M/r$. Substituting this into equation (12), we find,

$$\hat{\alpha} = -\frac{2G_N M x}{c^2} \int_{y_S}^{y_O} \frac{dy}{(x^2 + y^2)^{3/2}} \Rightarrow$$

$$\hat{\alpha}(\xi) = \frac{4G_N M}{c^2 \xi} \quad (13)$$

Where ξ is the impact parameter, or alternatively the closest distance of the light ray to the mass M . It was this deflection angle that enabled Eddington[7] to confirm Einsteins theory of general relativity for the first time. The deflection angle $\hat{\alpha}$ depends on the impact parameter ξ . It is this dependence that allows us to view $\hat{\alpha}$ as the deflection map, giving the deflection of a distant source as a function of apparent position in the sky. Let us turn our attention to the general geometrical setting for gravitational lensing.

Galaxy–Galaxy lensing

In figure 2 the typical situation is drawn. The observer O detects the light of a distance source S . This source has a two dimensional position $\vec{\eta}$ in

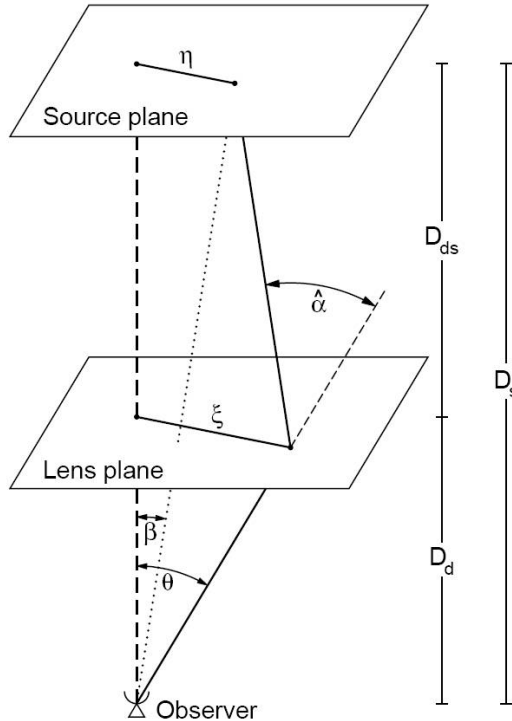


Figure 2: The typical arrangement in gravitational lensing. With a source plane, lensing plane and an observer. The mass distribution around the lensing plane bends the light of the sources such that the observer sees the sources at another position. In practice the effects will be magnification and distortion of the source galaxies. This image is taken from [10].

the source plane. A light ray emitted by the source gets deflected in the lens plane by some mass distribution at position $\vec{\xi}$ and traverses to the observer. Suppose that we have a three dimensional mass distribution $\rho(\vec{r})$ in the neighborhood of the lens plane. In the neighborhood here means that ρ should not be extended from source plane to observer. This condition is satisfied in almost all astrophysical situations, because the typical size of a cluster of galaxies is a few Mpc, whereas the distances between observer and source plane are of the order of the Hubble length $\approx 3h^{-1}10^3\text{Mpc}$. This argument allows us to make a thin-lens approximation. This approximation projects all lensing mass onto a two-dimensional plane, the lensing plane. Since we are dealing with weak gravitational lensing here, we are only interested in first order lensing effects. So we make an approximation that is similar to the Born approximation of quantum mechanics. Using equation (11) we can deduce how the deflection field $\hat{\alpha}(\vec{\xi})$ depends on the vector $\vec{\xi}$. For our three dimensional mass distribution $\rho(r)$, we insert the Newtonian

potential,

$$\phi_N(\vec{r}) = -G \int d^3r' \frac{\rho(\vec{r}')}{|\vec{r} - \vec{r}'|} = -G \int dr' \int d^2\vec{\xi}' \frac{\rho(r', \vec{\xi}')}{|\vec{r} - \vec{\xi}'|}, \quad (14)$$

where $\vec{\xi}'$ in the last equality is defined as $(r', \xi'_1, \xi'_2)^T$. Analogous to (11) we find,

$$\frac{d\vec{\xi}(y)}{dt} = \frac{2G}{c} \int_{y_S}^y dy' \int dr' \int d^2\vec{\xi}' \vec{\nabla}'_{\perp} \frac{\rho(r', \xi'_1, \xi'_2)}{\left((y' - r')^2 + (\vec{\xi} - \vec{\xi}')^2\right)^{1/2}} = \quad (15)$$

$$= \frac{2G}{c} \int_{y_S}^y dy' \int dr' \int d^2\vec{\xi}' \frac{-\rho(r', \xi'_1, \xi'_2)(\vec{\xi} - \vec{\xi}')}{\left((y' - r')^2 + (\vec{\xi} - \vec{\xi}')^2\right)^{3/2}}. \quad (16)$$

Now we perform the integration $\int_{y_S}^y dy'$ to obtain,

$$\hat{\alpha}(\vec{\xi}) = \frac{4G_N}{c^2} \int d^2\vec{\xi}' \int dr' \rho(\xi'_1, \xi'_2, r') \frac{\vec{\xi} - \vec{\xi}'}{|\vec{\xi} - \vec{\xi}'|^2}. \quad (17)$$

This $\hat{\alpha}$ is now a two dimensional deflection angle at each impact parameter $\vec{\xi}$. The integration over r' is the integration over spatial dimension perpendicular to the deflection plane. Now we introduce the surface mass density,

$$\Sigma(\vec{\xi}) = \int dr' \rho(\xi_1, \xi_2, r'). \quad (18)$$

This allows us to write (17) as,

$$\hat{\alpha}(\vec{\xi}) = \frac{4G_N}{c^2} \int d^2\vec{\xi}' \Sigma(\vec{\xi}') \frac{\vec{\xi} - \vec{\xi}'}{|\vec{\xi} - \vec{\xi}'|^2}. \quad (19)$$

From the above equation it seems that all information about the mass distribution in the direction perpendicular to the lensing plane is integrated out. We will come back on this matter. In fact, the surface mass density has a redshift dependency that allows us to break the mass sheet degeneracy. We require an equation relating the apparent position of the source to the true position of the source. From Fig. 2 it is easy to see that

$$\vec{\eta} = \frac{D_s}{D_d} \vec{\xi} - D_{ds} \hat{\alpha}(\vec{\xi}). \quad (20)$$

Furthermore we introduce angular coordinates by $\vec{\eta} = D_s \vec{\beta}$ and $\vec{\xi} = D_d \vec{\theta}$. Now we can rewrite (20) into,

$$\vec{\beta} = \vec{\theta} - \frac{D_{ds}}{D_s} \hat{\alpha}(D_d \vec{\theta}) \equiv \vec{\theta} - \vec{\alpha}(\vec{\theta}), \quad (21)$$

where in the last step we rescaled the deflection angle $\hat{\alpha} \rightarrow \vec{\alpha}$. The interpretation is now as follows. A source at position $\vec{\beta}$ can be seen by an observer at angular positions $\vec{\theta}$ when (21) is satisfied. For some matter distributions (21) has multiple solutions for fixed $\vec{\beta}$, this only happens when we are dealing with strong lenses. The strength of a lens can be quantified using the dimension-less surface mass density,

$$\kappa(\theta) = \frac{\Sigma(D_d \vec{\theta})}{\Sigma_{cr}} \text{ with } \Sigma_{cr} = \frac{c^2}{4\pi G_N} \frac{D_s}{D_d D_{ds}}. \quad (22)$$

Where Σ_{cr} denotes the critical surface mass density. In the following we neglect the fact that the dimension-less surface mass density $\kappa(\theta)$ is also dependent on the redshift of the lens and source. We will return to this point at a later time. When $\kappa(\theta) \geq 1$ multiple images can occur, such as Einstein rings and arcs. Although strong gravitational lensing is interesting on its own, we will not go into it here. We will only consider mass distributions that give rise to weak lensing. We are able to express the rescaled deflection angle $\vec{\alpha}$ in terms of the dimension-less surface mass density $\kappa(\theta)$,

$$\vec{\alpha}(\vec{\theta}) = \frac{1}{\pi} \int_{\mathbb{R}^2} d^2\theta' \kappa(\vec{\theta}') \frac{\vec{\theta} - \vec{\theta}'}{|\vec{\theta} - \vec{\theta}'|^2}. \quad (23)$$

In the above equation we recognize the Green's function of the Poisson equation. This implies that we can introduce a *deflection potential* Ψ . This potential will have the property that $\vec{\alpha} = \nabla \Psi$, where ∇ is the gradient operator in the $\vec{\theta}$ plane. The deflection potential can be written as,

$$\Psi(\vec{\theta}) = \frac{1}{\pi} \int_{\mathbb{R}^2} d^2\theta' \kappa(\vec{\theta}') \log |\vec{\theta} - \vec{\theta}'|. \quad (24)$$

With this potential, we are ready to express the apparent position of the source in terms of the original position. Suppose that the source has an surface brightness distribution $I^s(\vec{\beta})$, and the apparent spot on the telescope has an surface brightness distribution $I(\vec{\theta})$. In the limit of small deflections, i.e. weak lensing, we have conservation of total surface brightness by Liouville's theorem, and the absence of other light emitting or absorbing sources we are allowed to write,

$$I(\vec{\theta}) = I^s(\vec{\beta}(\vec{\theta})), \quad (25)$$

where we used the lens equation (21). When the angular size of the source is smaller than the size on which the lens properties change, we can approximate equation (25) using a linear approximation for $\vec{\beta}$ in $\vec{\theta}$,

$$I(\vec{\theta}) \approx I^s \left(\vec{\beta}_0 + \mathcal{A}(\vec{\theta}_0) \cdot (\vec{\theta} - \vec{\theta}_0) \right), \quad (26)$$

where \mathcal{A} is the Jacobian matrix of the lensing map. We have,

$$\mathcal{A}(\vec{\theta}) = \frac{\partial \vec{\beta}}{\partial \vec{\theta}} = \begin{pmatrix} 1 - \kappa - \gamma_1 & -\gamma_2 \\ -\gamma_2 & 1 - \kappa + \gamma_1 \end{pmatrix}. \quad (27)$$

In this expression we recognize $\kappa(\theta)$ as the dimensionless surface mass density. The components of the shear γ that appear in the above equation are defined as linear combinations of first order derivatives of the deflection potential,

$$\gamma_1 = \frac{1}{2}(\Psi_{,11} - \Psi_{,22}) \quad (28)$$

$$\gamma_2 = \Psi_{,12}. \quad (29)$$

In the above expression we used the notation $\Psi_{,12} = \partial_{\theta_1} \partial \theta_2$, where θ_1 and θ_2 are components of the vector $\vec{\theta}$. The shear forms a traceless, symmetric 2×2 -matrix. We can identify this kind of matrix one-to-one with a complex number so we can write the shear as $\gamma = \gamma_1 + i\gamma_2 = |\gamma| e^{2i\phi}$. Note the factor of two in front of the angle ϕ . This implies that the shear does not correspond to a vector, as can be seen by performing a coordinate transformation. A rotation over π results in the same ellipse, which is what had to be expected from the symmetries of an ellipse.

When $\vec{\theta}_0$ is a point in the image, that corresponds with $\vec{\beta}_0 = \vec{\beta}(\vec{\theta}_0)$ in the source, then the lensing is governed by the linearized lens equation (26). This equation projects circular objects to elliptical ones. The inverses of the eigenvalues of $\mathcal{A}(\vec{\theta}_0)$ correspond to the ratios of the semi-axes of these ellipses to the radius of the source. These inverse eigenvalues are $-\lambda_{1,2} = 1 - \kappa \pm |\vec{\gamma}|$. The observed fluxes from both the observed and unlensed source can be obtained by integrating the brightness distributions I and I^s . The magnification $\mu(\vec{\theta}_0)$ is given by the ratio of the two brightness distributions and can be written as,

$$\mu = \frac{1}{\det(\mathcal{A})} = \frac{1}{(1 - \kappa)^2 - |\gamma|^2}. \quad (30)$$

From this equation it is clear that the magnification diverges for $(1 - \kappa)^2 = |\gamma|^2$. When this happens we are close to critical curves called *caustics*. Near those curves the weak lensing approximation we used is no longer valid. This is exactly the place where we have to switch to a strong lensing description. Those caustics then correspond to Einstein arcs. The deflection of the light by the mass distribution thus induces two effects on the distribution of the surface brightness. The first effect is distortion due to a tidal gravitational potential. The second effect is magnification due to isotropic focusing of the light rays by the matter distribution κ . The magnification is also caused by anisotropic focusing of the shear.

Observables

Now that we have written down the linearized lensing equation we are ready to introduce the framework of weak lensing. In the last section we started from the mass distribution and derived the map that describes the deflection of light from it. In practice, it is the matter distribution that we want to measure. So we have to work our way back inverting the equations above. However, there is another problem in weak lensing. That is, we do not know the surface brightness distribution of the sources $I^s(\vec{\beta})$. The only thing we know from our measurements is the observed brightness distribution $I(\vec{\theta})$. To be able to make some further progress we approximate the shape of all observed and source galaxies by ellipses. In this way we will be able to analyze the lensing map, and deduce the mass distribution from it. We proceed by introducing some new quantities, that quantify the size and ellipticity of observed objects. First let us define what we call the center of an observed galaxy. The center of an observed galaxy is defined as,

$$\vec{\theta}^c \equiv \frac{\int d^2\theta w_I(I(\vec{\theta})) \vec{\theta}}{\int d^2\theta w_I(I(\vec{\theta}))} \quad (31)$$

In this expression $w_I(I)$ is a suitable weight function. Suitable means that is chosen such that the integrals converge. For example the weight function $w_I(I) = H(I - I_{cutoff})$, with H the Heaviside step function, implies that $\vec{\theta}^c$ is the center of the area enclosed by the cutoff isophote I_{cutoff} . After a suitable $w_I(I)$ is chosen we can define the tensor of second brightness moments,

$$Q_{ij} = \frac{\int d^2\theta w_I(I(\vec{\theta})) (\theta_i - \theta_i^c)(\theta_j - \theta_j^c)}{\int d^2\theta w_I(I(\vec{\theta}))}. \quad (32)$$

With these definitions made we can now define what we mean by the size and ellipticity of an object. We define the size of an object as,

$$\omega = (Q_{11}Q_{22} - Q_{12}^2)^{1/2}. \quad (33)$$

This definition is such that for the weight function we mentioned as example, the size is proportional to the solid angle enclosed by the cutoff isophote. For

the shape of the object we introduce the object called the complex ellipticity,

$$\chi = \frac{Q_{11} - Q_{22} + 2iQ_{12}}{Q_{11} + Q_{22}}. \quad (34)$$

If the image has elliptical isophotes, and the axes have a ratio $r \leq 1$, then the complex ellipticity $\chi = (1 - r^2)(1 + r^2)^{-1} \exp(2i\vartheta)$. The phase of χ is two times the position angle ϑ of the major axis. We can make equivalent definitions for the source surface brightness distribution I^s . So we can again define the center $\vec{\beta}^c$ and the tensor of second brightness moments Q_{ij}^s . Now comes the crucial step. We use the linearized lens equation (26) to obtain,

$$Q^s = \mathcal{A}Q\mathcal{A}^T = \mathcal{A}Q\mathcal{A}, \quad (35)$$

with $\mathcal{A} = \mathcal{A}(\vec{\theta}^c)$. We used the symmetry of the Jacobian matrix in the last equality. From this relation we can deduce the relation between the observed and true complex ellipticity,

$$\chi^s = \frac{\chi - 2g + g^2\chi^*}{1 + |g^2| - 2\mathcal{R}e(g\chi^*)}, \quad (36)$$

where we introduced the notion of the reduced shear g , which is defined as,

$$g(\vec{\theta}) = \frac{\gamma(\vec{\theta})}{1 - k(\vec{\theta})}. \quad (37)$$

When we want to know χ as a function of χ^s , i.e. the inverse of equation (36), all that we have to do is replacing them in equation (36), and replace g by $-g$. It is evident from equation (36) that the transformation of the complex ellipticities depends only on the reduced shear. It does not depend on the complex shear and surface mass density separately. This can also be seen by writing equation (27) as,

$$\mathcal{A} = (1 - \kappa) \begin{pmatrix} 1 - g & -g \\ -g & 1 + g \end{pmatrix} \quad (38)$$

The prefactor $1 - \kappa$ only affects the size of the image, but does not distort the image, leaving the shape invariant. From equation (35) it is evident that the size ω , defined in equation (33), transforms under lensing as,

$$\omega = \mu(\vec{\theta})\omega^s. \quad (39)$$

Now that we have derived the transformation properties of both the size and the shape of the objects, we would like to move on and look how we can use these results to probe the mass distribution of the lensing matter. In the beginning of this section we pointed out that we do not know *a priori* what the orientation or size of a distant source galaxy is. A single

measurement on one galaxy provides no knowledge about the strength of the intermediate lens. Nor does it provide information over the strength of the tidal field, because our lack of information about the intrinsic complex ellipticity of the source galaxy. So we have to rely on statistics. We assume that all faint source galaxies that appear in the neighborhood of position $\vec{\theta}$ are randomly oriented. The galaxies should be close to the point $\vec{\theta}$ to be able to assume that the lensing properties, so κ and γ , do not change significantly in this neighborhood. We assume that the expectation value of the complex ellipticities vanishes,

$$E(\chi^s) = 0. \quad (40)$$

This assumption is a quite weak one. We have to realize that we are dealing with galaxies that are far away, at the order of the Hubble scale. Although they appear close to $\vec{\theta}$ their real spatial separation will be large. The assumption is further supported by deep space observations of the Hubble telescope, giving a weak two-point angular auto-correlation. We mentioned that a circular source will be mapped to an elliptical image. The ellipticity of this image determines the ratio of the eigenvalues of the Jacobian \mathcal{A} . For an ensemble of galaxies with a vanishing expectation value the same holds. From equation (38) we can consider the ratio,

$$r = \frac{1 \mp |g|}{1 \pm |g|}. \quad (41)$$

Here we can see something interesting. The ratio $r \rightarrow -r$ under substitution $g \rightarrow 1/g^*$, in other words the magnitude of r is the same for g and $1/g^*$. The sign of r cannot be recovered from local measurements. This implies that we cannot discern g from $1/g^*$. This is called *local degeneracy*. This means that we can only measure functions of g that are invariant under $g \rightarrow 1/g^*$. For instance the *complex distortion*,

$$\delta \equiv \frac{2g}{1 + |g|^2}. \quad (42)$$

After the replacement of the expectation value of equation (40) by the average over a local ensemble ellipticities, $\langle \chi^s \rangle \approx E(\chi^s) = 0$. Then we can find an equation to determine the complex distortion δ , following Schneider & Seitz [8], we define,

$$\chi_+^s \equiv \chi^s(g) + \chi^s(1/g^*) = \frac{2f + \chi + \chi^* \delta / \delta^*}{1 + \mathcal{R}e(\delta \chi^*)} \quad (43)$$

$$\chi_-^s \equiv \chi^s(g) - \chi^s(1/g^*) = \left(\frac{1 - |g|^2}{1 + |g|^2} \right) \frac{\chi - \chi^* \delta / \delta^*}{1 + \mathcal{R}e(\delta \chi^*)} \quad (44)$$

Now we find that the combination,

$$C := \frac{1}{2} \left(\chi_+^s + \frac{1 - |g|^2}{1 + |g|^2} \chi_-^s \right) = \frac{\delta \chi}{1 + \mathcal{R}e(\delta \chi^*)}, \quad (45)$$

depends only on δ , and because $\langle \chi^s(g) \rangle = \langle \chi^s(1/g^*) \rangle = 0$. The relation to determine δ becomes,

$$N \langle C \rangle = \sum_{i=1}^N \frac{\delta + \chi_i}{1 + \mathcal{R}e(\delta \chi_i^*)} = 0. \quad (46)$$

Now we can search the root of this equation. There is however another approach. We can solve for δ using the iteration equation,

$$\delta_{n+1} = - \left\langle \frac{\chi}{1 + \mathcal{R}e(\delta_n \chi^*)} \right\rangle \left(\left\langle \frac{1}{1 + \mathcal{R}e(\delta_n \chi^*)} \right\rangle \right)^{-1}, \quad (47)$$

where we start with $\delta_0 = -\langle \chi \rangle$. With these definitions we converge fast towards our desired δ . This distortion is an unbiased estimate of the distortion in the image. Its dispersion about the true value depends on the dispersion σ_χ of the intrinsic ellipticity distribution. An estimate for the *rms* error of δ is $\sigma_\delta \approx \sigma_\chi N^{-1/2}$, where N is the number of galaxies that is used for the local average. This estimate is quite accurate, but it overestimates the error for large $|\delta|$ [8]. The estimates for δ and g as introduced above can be derived without knowledge about the intrinsic distribution of the ellipticities of the source galaxies. When this distribution is explicitly known, from other measurements, we can exploit this extra knowledge. With this information we can determine both δ and g through a maximum-likelihood method. In the case of weak gravitational lensing, the case we are interested in, we have $k \ll 1$ and $|\gamma| \ll 1$. Which implies that $|g| \ll 1$. From equations (40) and (46) we find,

$$\gamma \approx g \approx \frac{\delta}{2} \approx \frac{\langle \chi \rangle}{2}. \quad (48)$$

Recall that the definition of the dimension-less surface mass density κ in equation (22) had a redshift dependency. Up to now we ignored this redshift dependency and assumed all sources to be at the same redshift. In other words we made the assumption that the ratio D_{ds}/D_s between the lens-source and observer-source distances is the same for all sources. Since the deflection angle, the deflection potential and the shear are all linearly dependent on κ . This means that the distance ratio D_{ds}/D_s is sufficient to specify the lens strength as a function of redshift. For $z_d \leq 0.2$ this ratio is fairly constant for sources at redshift $z_s \geq 0.8$, so our previous approximation applies to relatively low-redshift deflectors. For lenses that are further away we have to take the redshift distribution of the sources into account.

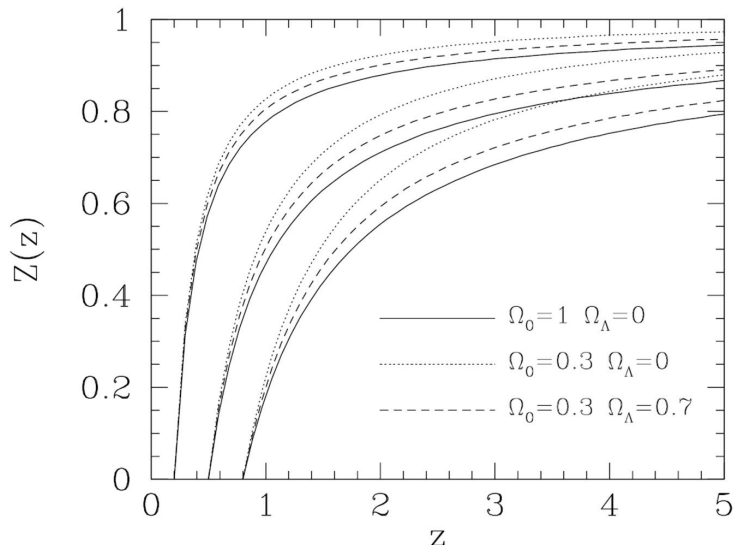


Figure 3: The function $Z(z)$ for three different cosmologies. The function describes the relative strength as a function of source redshift. For each choice of the cosmological parameters, three different lens redshifts are plotted, $z_d = 0.2, 0.5, 0.8$. From the definition in (49) we see $Z(z) \rightarrow 0$ as $z \rightarrow z_d$, and $Z(z) \rightarrow 1$ as $z \rightarrow \infty$. For sources close to the lens $Z(z)$ varies strongly, but depends relatively weakly on cosmology.

For a lens at redshift z_d , the dimensionless surface mass density and the complex shear are functions of the source redshift. Let us define,

$$Z(z) \equiv \frac{\lim_{z \rightarrow \infty} \Sigma_{cr}(z_d, z)}{\Sigma_{cr}(z_d, z)} H(z - z_d) = \frac{f_R(r(z_d, z)) f_R(r(0, \infty))}{f_R(r(0, z)) f_R(r(z_d, \infty))} H(z - z_d). \quad (49)$$

The Heaviside step function makes sure that objects that are closer to us than the lens are not lensed. The function $f_R(r)$ determines whether we live in a closed, flat or open universe. Now we can define $\kappa(z, \vec{\theta}) = Z(z)k(\vec{\theta})$, and likewise $\gamma(\vec{\theta}, z) = Z(z)\gamma(\vec{\theta})$ for a source at z , and κ and γ refer to a source at redshift infinity. In figure 3 the function depending on redshift $Z(z)$ is plotted for different cosmologies. The figure is taken from [10].

Before we proceed with the analysis of the impact the redshift dependency has we introduce another measure for the complex ellipticities. This measure is equivalent to χ but is more convenient to work with. We define the complex ellipticity ϵ as,

$$\epsilon = \frac{Q_{11} - Q_{22} + 2iQ_{12}}{Q_{11} + Q_{22} + 2(Q_{11}Q_{22} - Q_{12}^2)^{1/2}}. \quad (50)$$

ϵ and χ are related as,

$$\epsilon = \frac{\chi}{1 + (1 - |\chi|^2)^{1/2}}, \quad \chi = \frac{2\epsilon}{1 + |\epsilon|^2}. \quad (51)$$

Like equation (36) relating the image and source ellipticities there is a relation between ϵ^s and ϵ see[11],

$$\epsilon^s = \begin{cases} \frac{\epsilon - g}{1 - g^* \epsilon} & \text{for } |g| \leq 1 \\ \frac{1 - g^* \epsilon}{\epsilon^* - g^*} & \text{for } |g| > 1 \end{cases} \quad (52)$$

Since ϵ is equivalent to χ and by equation (51) it is easy to see that $\langle \epsilon^s \rangle \approx E(\epsilon^s) = 0$. The expectation value of the observed ellipticity ϵ as a function of redshift is given by,

$$E[\epsilon(z)] = \begin{cases} \frac{Z(z)\gamma}{1 - Z(z)\kappa} & \text{for } \mu(z) \geq 0 \\ \frac{1 - Z(z)\kappa}{Z(z)\gamma^*} & \text{for } \mu(z) < 0 \end{cases}, \quad (53)$$

where the magnification $\mu(z)$ as function of the source redshift can now be written as,

$$\mu(z) = ((1 - Z(z)\kappa)^2 - Z^2(z) |\gamma|^2)^{-1}. \quad (54)$$

Now we are ready to consider the following case. In this case we assume that we know the redshift distribution of the sources. We define the probability $p_z(z)dz$ that a galaxy image has a redshift within dz of z . In general, the observed redshift distribution will be different than the true redshift distribution of the sources. This comes from the fact that magnified sources can be seen up to higher redshifts than unlensed ones. We can expect that the redshift distribution we observe will depend on the local lens parameters κ and γ that determine the magnification (54). For small magnifications or for redshift distributions that depend weakly on the flux, the observed and true redshift distributions can be identified. Given the distribution $p_z(z)$, the expectation value of the image ellipticity becomes,

$$E(\epsilon) = \int dz p_z(z) E[\epsilon(z)] = \gamma \left[X(\kappa, \gamma) + |\gamma|^{-2} Y(\kappa, \gamma) \right], \quad (55)$$

which is just a weighted average. The two functions X and Y of κ and γ that appear in the last identity are given by,

$$X(\kappa, \gamma) = \int_{\mu(z) \geq 0} dz p_z(z) \frac{Z(z)}{1 - Z(z)\kappa}, \quad (56)$$

$$Y(\kappa, \gamma) = \int_{\mu(z) < 0} dz p_z(z) \frac{1 - Z(z)\kappa}{Z(z)}, \quad (57)$$

where the integration boundaries depend on $\mu(\kappa, \gamma)$. We can make distinction between different lenses. When $\mu(z) > 0$ for all z the lens is said to

be sub-critical. This condition is equivalent to $1 - \kappa - |\gamma| > 0$. We can immediately see from equation (57) that for sub-critical lenses $Y = 0$. This implies that $E(\epsilon) = \gamma X(\kappa, \gamma)$. In [11] an approximation is derived for the case $\kappa \leq 0.6$,

$$\gamma = \frac{E(\epsilon)}{\langle Z \rangle} \left(1 - \frac{\langle Z^2 \rangle}{\langle Z \rangle} \kappa \right), \quad (58)$$

where $\langle Z^n \rangle \equiv \int dz p_z(z) Z^n$. Now for the weak lensing case, we can approximate this expression even further. We have,

$$E(\epsilon) \approx \langle Z \rangle \gamma. \quad (59)$$

This means that when we are dealing with weak gravitational lensing we can collapse the source redshift distribution into a single redshift z_s that must satisfy $Z(z_s) = \langle Z \rangle$. When we now replace $E(\epsilon)$ by $\langle \epsilon \rangle$ we have an estimation of the shear $\gamma^1 = \langle \epsilon \rangle / \langle Z \rangle$ in the weak lensing case.

Let us define the number of galaxy images per unit solid angle in the absence of lensing as $n_0(S, z)dz$ with a flux within dS of S and redshift within dz of z . When we are observing at a point $\vec{\theta}$ the number density can be changed by the magnification at that point. Images of a set of sources are distributed over a larger solid angle which reduces the observed number density by a factor $\mu^{-1}(z)$. But remember that magnification allows the observation of fainter sources. Adding up these effects we arrive at an expected number density,

$$n(S, z) = \frac{1}{\mu^2(z)_0} \left(\frac{S}{\mu(z)}, z \right), \quad (60)$$

where the magnification $\mu(z)$, given by equation (54), depends on κ and γ . From the above relationship we can deduce the redshift distribution,

$$p(z; S, \kappa, \gamma) = \frac{n_0 [\mu^{-1}(z)S, z]}{\mu^2(z) \int dz' \mu^{-2}(z') n_0 [\mu^{-1}(z)S, z]}. \quad (61)$$

This function can now be substituted for $p_z(z)$ in eq. (55).

Now suppose that we do know the redshifts of the source galaxies. Although this may seem a bold assumption, due to detailed photometric measurements it is not. These measurements can achieve an accuracy of about $\Delta z \approx 0.1$. This uncertainty is small compared to scale of the variations of $Z(z)$. This means that we can treat those measurements as if they were precise. If now the redshifts z_i of our source galaxies are known we can estimate the shear, in the weak lensing regime,

$$\gamma^2 = \frac{\sum_i u_i Z_i \epsilon_i}{\sum_i u_i Z_i^2}. \quad (62)$$

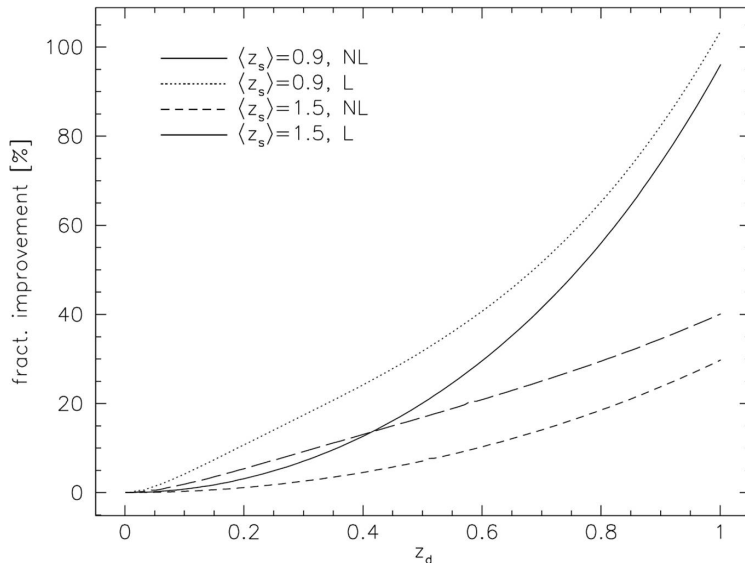


Figure 4: The fractional accuracy gain in the shear estimate due to the knowledge of the source redshift, more precisely the deviation from unity in per cent of the ratio of the dispersions. The four curves correspond to two different mean source redshift. And to cases without lensing(NL), ($\kappa = \gamma = 0$), and with lensing(L), ($\kappa = .3 = |\gamma|$). With the assumption of an Einstein–de Sitter cosmology. As expected, the higher the lens redshift z_d , the more substantially is the shear estimate improved by knowledge of the redshifts, since for low z_d the function $Z(z)$ is almost constant. The lower mean redshift of the source distribution, the more important the knowledge of the redshifts becomes. Finally redshift information is relatively more important for larger lens strength. This image is taken from [10].

When we now compare the uncertainties of the shear estimates for the case where we do not know the distribution of the source galaxies γ^1 and where we do know the redshifts γ^2 . For a detailed derivation see [10]. In figure 4 we can quantitatively compare the gain in accuracy due to knowledge of the redshift distribution of the source galaxies. The figure makes clear to us that the accuracy of the estimation of the shear is significantly improved by the knowledge of the source redshift. This holds in particular when the lens redshift is a fair fraction of the mean source distance. Although the figure is created using some crude approximations, namely that there were only small correlations in redshift for the source galaxies, which can be doubted, we have to accept the conclusion that knowledge on the redshifts of the source galaxies greatly enhances the accuracy of weak lensing results.

Now we will turn our attention on another effect that could be measured. It is the magnification caused by the lens that we can use to determine the lens properties. In the above we looked at image distortions of the

ellipticities of the source galaxies. We will look in detail into the change in the number density of galaxies. Let $n_0(> S, z)dz$ be the number density of galaxies with redshift within dz of z and with a flux larger than S . Now at some position $\vec{\theta}$ we can write for the number counts according to (60),

$$n(> S, z) = \frac{1}{\mu(\vec{\theta}, z)} n_0 \left(> \frac{S}{\mu(\vec{\theta}, z)} \right). \quad (63)$$

This equation implies that magnification effects can either increase or decrease the local number of counts. This depends on the shape of the unlensed number–count function. This change of number counts is called *magnification bias*, and is important for gravitational lensing of QSOs. As stated earlier, magnification allows the observation of fainter sources. We have,

$$p(z; > S, \kappa, \gamma) = \frac{n_0 [> \mu^{-1}(z)S, z]}{\mu(z) \int dz' \mu^{-1}(z')S, z'}, \quad (64)$$

which is in analogy to equation (61) at fixed flux. Since we are dealing with very faint objects here, spectroscopic information is hard to obtain. Therefore one can only observe the redshift–integrated counts,

$$n(> S) = \int dz \frac{1}{\mu(z)} n_0(> \mu^{-1}(z)S, z). \quad (65)$$

From observational evidence it follows that the number counts of faint galaxies closely follow a power law over a wide range of fluxes. This allows us to write the unlensed counts as,

$$n_0(> S, z) = \alpha S^{-\alpha} p_0(z; S), \quad (66)$$

where the exponent α depends on the wave band of the observation, and $p_0(z; S)$ is the redshift probability distribution of galaxies with flux $> S$. The ratio of the lensed and unlensed source counts is then found by inserting the power law behavior of the unlensed number density into the redshift integrated counts,

$$\frac{n(> S)}{n_0(> S)} = \int dz \mu^{\alpha-1}(z) p_0(z; \mu^{-1}S). \quad (67)$$

Note that the lensed counts do not strictly follow a power law in S , since p_0 depends on z . The redshift distribution $p_0(z, S)$ is currently unknown, therefore the change of the number counts due to the magnification cannot be predicted. For faint flux thresholds the redshift distribution is likely to be dominated by galaxies at relative high redshift. For lenses at fairly small redshift of about $z_d \leq 0.3$, we can approximate the redshift–dependent

magnification by the magnification μ of a fiducial source at infinity, in which case,

$$\frac{n(> S)}{n_0(> S)} = \mu^{\alpha-1}, \quad (68)$$

which gives us a local estimation of the magnification. In the absence of shape information and in the limit of weak gravitational lensing we have $\mu \approx (1 + 2\kappa)$ and we can obtain an estimate of the surface mass density,

$$\kappa \approx \frac{n(> S) - n_0(> S)}{n_0(> S)} \frac{1}{2(\alpha - 1)}. \quad (69)$$

Now that we have two independent methods to obtain estimates about the mass distribution in the lensing plane it is interesting to compare those two methods. Thus, we are going to compare the method that is based on shear measurements, and the one based on the number of counts. Consider a small patch of the sky that contains N galaxy images in the absence of gravitational lensing. The patch that we are considering must be sufficiently small to make sure that the lens parameters can be assumed to be constant. The dispersion of a shear estimate from averaging over galaxy ellipticities is σ_ϵ^2/N so that the signal-to-noise ratio is,

$$\left(\frac{S}{N}\right)_{shear} = \frac{|\gamma|}{\sigma_\epsilon} \sqrt{N}. \quad (70)$$

According to equation (69), the expected change in galaxy number counts is $|\Delta N| = 2\kappa |\alpha - 1| N$. Assuming Poissonian noise, the signal-to-noise ratio in this case is,

$$\left(\frac{S}{N}\right)_{counts} = 2\kappa |\alpha - 1| \sqrt{N}. \quad (71)$$

Upon comparison we find,

$$\frac{(S/N)_{shear}}{(S/N)_{counts}} = \frac{|\gamma|}{\kappa} \frac{1}{2\sigma_\epsilon |\alpha - 1|}. \quad (72)$$

For situations such that $\kappa \approx |\gamma|$, the above equation implies that the signal-to-noise ratio of the shear measurement is considerably larger than that of the magnification. Even for number-count slopes as flat as $\alpha \approx 0.5$, this ratio is larger than five, with $\sigma_\epsilon \approx 0.5$. This leads us to conclude that shear measurements yield more significant results than magnification measurements. But there is more to this. Let make some additional considerations. Another argument to favor the shear measurements over the magnification measurements is that we have a precise expectation in the absence of lensing for the shear measurements. The other method needs to compare the

measurements with calibration fields that are not lensed, which requires accurate photometry. Second, equation (71) overestimates the signal-to-noise ratio since we assumed errors in a Poisson-like fashion. But real galaxies are known to cluster even at very faint magnitudes, and so the error is underestimated. This is why most weak lensing measurements are done using galaxy ellipticities.

Observations

Now we are going to discuss some observations based on gravitational lensing. First, we will discuss the observations made by Clowe et al.[13], that used weak gravitational lensing to prove the existence of dark matter directly. The second we are going to discuss by Massey et al.[14]. This paper deals with large scale three-dimensional structures in the universe. The three-dimensional maps are created using weak gravitational lensing analysis.

A direct empirical proof of the existence of dark matter

In this section we discuss an application of the theory we have outlined in the preceding section. The article by Clowe et al.[13] claims to have found direct empirical evidence that dark matter exists. And no alterations to the gravitational force law are needed. They present weak lensing measurements of 1E0657-558 ($z = 0.296$), also known as the Bullet Cluster. This system exhibits an unique feature. It consists of two galaxy clusters that are merging. During the merger of the two clusters the individual galaxies behave as collisionless particles. But the intracluster gas that is existent in both clusters, experiences ram pressure. This implies that during a collision the gas and galaxies will decouple spatially. This effect can clearly be seen in figure 5 of the Bullet Cluster. The geometry of this cluster provides a good opportunity to test the dark matter hypothesis using weak gravitational lensing. As described in the above weak gravitational lensing is capable of tracing the mass distribution of the lensing cluster. We can now discriminate between two different cases. The first case is without dark matter. Without dark matter the gravitational potential will be dominated by the mass of the colliding gas. For the second case, where dark matter is conjectured, we expect that weak lensing will show that the gravitational potential follows the distribution of the cluster cores. This because dark matter will behave as collisionless matter. In their paper Clowe et al. use shear measurements to reconstruct the dimension-less surface mass density κ . The peaks in the κ reconstruction are 8σ away from the centers of the plasma clouds. The orientation of those peaks is skewed towards the centers of the plasma peaks due to the fact that the plasma contributes about 10%

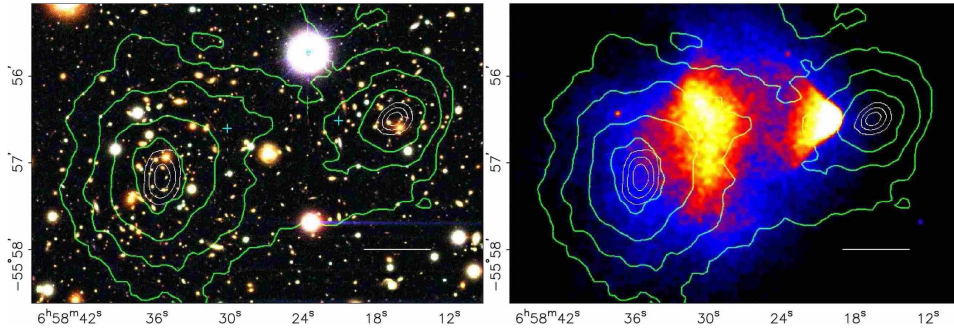


Figure 5: The Bullet Cluster, 1E0657–558. In the left panel is a color image from the Magellan telescopes. The right panel is a 500 ks Chandra image of the cluster showing the X–ray emission from the hot gas. In both panels the white bar indicates 200 kpc at the distance of the cluster. Also shown in both panels are reconstructed κ contour levels. These contours, obtained from weak lensing observations, correspond to $\kappa = 0.16$ in the outer contour and in increasing steps of $\kappa = 0.07$ towards the centers. The white contours indicate the errors on the positions of the κ peaks. The contours correspond to 68.3%, 95.5% and 99.7% confidence levels. The two +s are added to mark the position of the centers of the plasma clouds. These images strongly suggest that the mass density follows the galaxy centers, thus favoring a scenario with dark matter. These images were taken from [13].

of the total cluster mass. Note that both the plasma mass and the stellar mass are obtained directly from X–ray and optical images. Therefore they are independent of any gravity of dark matter model. Within the standard cosmological framework including dark matter the observed κ distribution is another piece of evidence for the existence of dark matter. But let us look at the possibility of explaining the observations on the Bullet Cluster within the MOND paradigm, or its relativistic extension TeVeS [4]. Within the TeVeS framework another κ map can be derived from the measurements. Without dark matter, the modifications to the theory of gravity should explain the discrepancy of location in both the plasma and galaxy peaks. Due to the geometry of the system TeVeS needs to postulate a disk of gas between the two mass concentrations that correspond to the subclusters. The measurements indicate that such a concentration is non–existent. This leads to the conclusion that every modified theory of gravity that scales with the baryonic mass fails to reproduce the correct results. In other words, in order to explain the observations modified gravity theories need to rely on additional dark matter. Concluding the paper ends with the justification of its title, the observed displacement between the bulk of the baryons and the gravitational potential proves the presence of dark matter for the most general assumptions regarding the behaviour of gravity.

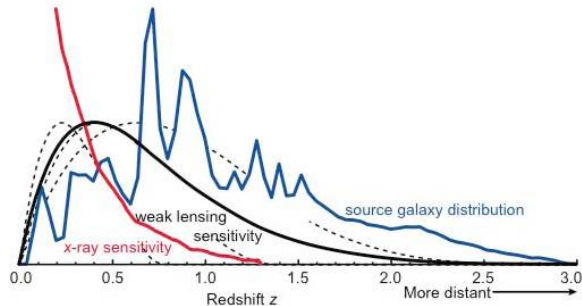


Figure 6: The redshift dependence of probes of large scale structure. The solid blue line represents the distribution of photometric redshifts for the source galaxies. The solid black line shows the sensitivity of weak lensing measurements. The red line shows the sensitivity of X-ray detections. Image taken from [14].

Breaking the mass sheet degeneracy

The largest part of this paper over weak gravitational lensing dealt with two dimensional reconstructions of the mass distribution in the lensing plane. There are methods to break free from this two dimensional flatland and explore three dimensional space. Here we are going to touch upon this subject. We proceed by discussing the paper by Massey et al.[14]. In the section where we outlined the basic theory describing weak gravitational lensing we already pointed out the fact that the dimension-less surface mass density κ is redshift dependent. This dependency we are going to exploit here to construct a three dimensional map of the (dark) matter distribution. Photometric redshift information about the source galaxies allows us to break the mass sheet degeneracy. In figure 6 the sensitivity of probes of large scale structure as a function of distance is showed. In order to create a 3D distribution of dark matter we have to put or source galaxies into redshift bins. The quality of the photometric information about the source galaxies allows us to put the source galaxies in redshift bins of $\Delta z = 0.05$. Shear measurements of the galaxies in these bins can be used to construct the κ map. Putting together all those slices yields a 3D image of the matter distribution. This distribution shows matter filaments in our universe. This matter distribution corresponds to the large scale distribution of baryonic matter. In figure 7 the distribution is shown. The two pictures that appeared in this section are taken from[14].

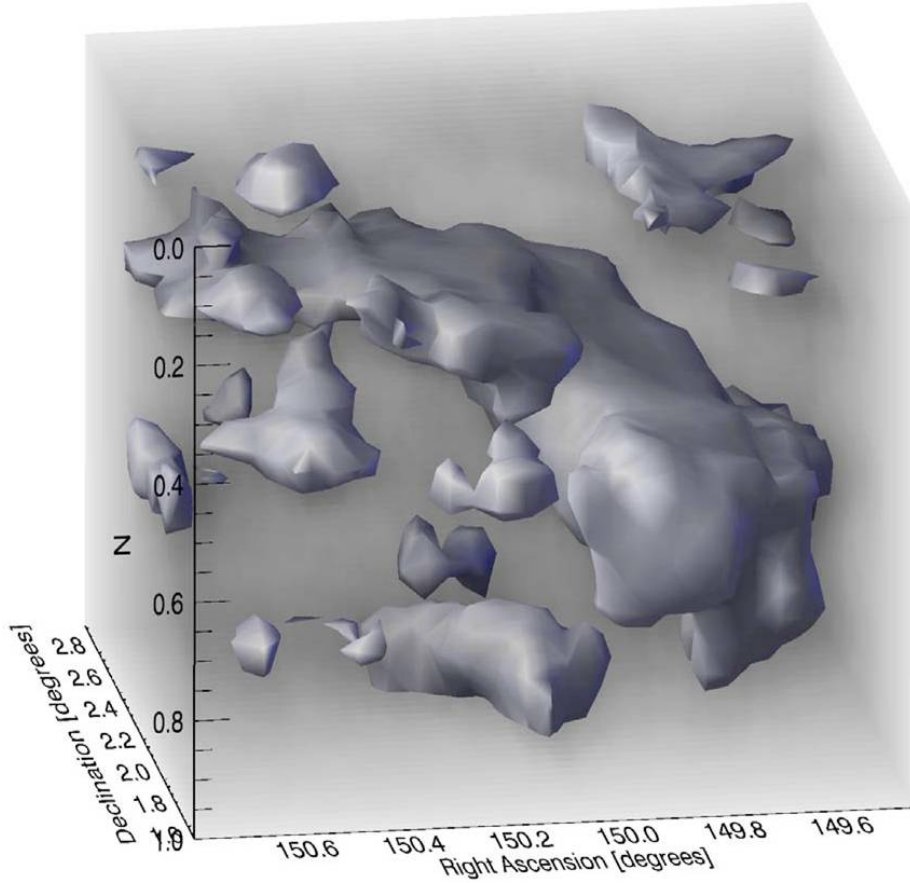


Figure 7: 3D reconstruction of the dark matter distribution. Axes correspond to Right Ascension, Declination, and Redshift. An isodensity contour has been drawn at a level of $1.6 \times 10^{12} M_{sun}$ within a circle of radius $700 kpc$. The image was constructed using redshift bins $\Delta z = 0.05$. The background grey scale corresponds to the local density. Image taken from [14].

Conclusion

In this paper we introduced the basic notions of weak gravitational lensing. The method of weak gravitational lensing is recognized to be one of the most reliable methods to determine the mass density of clusters. The reliability of this method comes from its freedom from assumptions about the physical state or the symmetries of the system. Next we introduced the deflection potential, the shear and magnification. We considered two methods to construct the dimensionless surface mass density. The first based on the increase in number density, the second on the shear. We showed that the method that was based on the shear measurements has a higher signal-to-noise ratio. Furthermore, the shear measurements do not need additional surveys of unlensed galaxies to compare with the lensed ones. Then we considered two papers that used the weak lensing shear analysis to draw conclusions that are cosmologically relevant. The first paper offered further proof that dark matter is real, and abundant in our universe. The other visualized the invisible dark matter and demonstrated that the distribution of dark matter shows similarities in structure with the visible baryonic mass distribution.

Notation and Conventions

The most general form of our metric has the form,

$$ds^2 = c^2 dt^2 - a^2(t) dl^2, \quad (73)$$

where dl is the line element of the homogeneous and isotropic three-space. A special case of (73) is the Minkowski metric where the scalefactor $a(t)$ is constant and dl is the Euclidean line element. The allowed form of the spatial line element is of the form,

$$dl^2 \equiv dr^2 + f_R^2(r)(d\phi^2 + \sin^2 \theta d\theta^2) \equiv dr^2 + f_R^2(r)d\Omega^2, \quad (74)$$

with,

$$f_R(r) = \begin{cases} R^{-1/2} \sin(R^{1/2}r) & R > 0 & \text{Open} \\ r & R = 0 & \text{Flat} \\ (-R)^{-1/2} \sinh((-R)^{1/2}r) & R < 0 & \text{Closed} \end{cases} . \quad (75)$$

Bibliography

- [1] Zwicky, F. 1933. Die Rotverschiebung von extragalaktischen Nebeln, *Helvetica Physica Acta* 6: 110127.
- [2] Rubin, V.C, Ford Jr WK. 1970. *Ap. J.* 159:379
- [3] Wayne Hu & Scott Dodelson. Cosmic Microwave Background Anisotropies. 2002. *Ann. Rev. A&A.* 40: 171–216. e-Print: Arxiv: Astro-ph/0110414.
- [4] Jacob. B. Bekenstein. The modified Newtonian dynamics–MOND and its implications for new physics. 2006. *Contemporary Physics* 47, 387. Arxiv: Astro-ph/0701848.
- [5] Thomas Rot, Modified Newtonian Dynamics: a possible solution to the dark matter problem, Seminar cosmology, 2009. e-Print: http://www.phys.uu.nl/~prokopec/ThomasRot_mond2.pdf
- [6] Tomislav Prokopec, Lecture notes on Cosmology I. 2007. e-Print: <http://www.phys.uu.nl/~prokopec/1gr.pdf>.
- [7] Dyson, F. Eddington, A. Davidson C. 1920. A Determination of the Deflection of Light by the Sun’s Gravitational Field, from Observations Made at the Total Eclipse of May 29, 1919. *Phil. Trans. Roy. Soc. A* **220**:291–333.
- [8] Schneider, P. & Seitz, C., Steps toward nonlinear cluster inversion through gravitational distortions, 1995, *A&A* **320**, 411.
- [9] Schneider P., Weak Gravitational Lensing, 2005, Arxiv:Astro-ph/0509252.
- [10] Bartelmann M. & Schneider P., Weak gravitational lensing, 2001, *Phys. Rept.* **340**, 291–472.
- [11] Seitz, C. & Schneider, P., 1997, *A&A*, **318**,687
- [12] Dipak Munshi, Patrick Valageas, Ludovic van Waerbeke, Alan F. Heavens, *Cosmology with Weak Lensing Surveys.* 2008, *Phys. Rept.* 462: 67–121. Arxiv:astro-ph/0612667.

- [13] Douglas Clowe, Marusha Bradac, Anthony H. Gonzalez, Maxim Markevitch, Scott W. Randall, Christine Jones and Dennis Zaritsky. A direct empirical proof of the existence of dark matter, 2006. *Astrophysical J.* **648** L109–L113. e-Print: <http://arxiv.org/abs/astro-ph/0608407>.
- [14] Richard Massey, Jason Rhodes, Richard Ellis, Nick Scoville, Alexie Leauthaud, Alexis Finoguenov, Peter Capak, David Bacon, Hervé Aussel, Jean-Paul Kneib, Anton Koekemoer, Henry McCracken, Bahram Mobasher, Sandrine Pires, Alexandre Refregier, Shunji Sasaki, Jean-Luc Starck, Yoshi Taniguchi, Andy Taylor & James Taylor. 2007. Dark matter maps reveal cosmic scaffolding, *Nature*, **445**: 286.